

# Iron Oxide Nanoparticles – Characterization and Antimicrobial Studies

Disholin Dennison Priya<sup>1</sup>, Thangavel Pichaiappa Rajesh<sup>1\*</sup>, Rachel Syam Sundar<sup>1</sup>, Chandrasekhar Narendhar<sup>2\*</sup>

<sup>1</sup>Department of Biotechnology, Anna University, Trichy, Tamil Nadu, India - 640024

<sup>2</sup>Department of Nanoscience and Technology, Sri Ramakrishna Engineering College, Coimbatore, Tamil Nadu, India - 641022

## ABSTRACT

Nanotechnology is one of the most promising technologies that give us better outcomes from biological and industrial issues. This work is mainly based on the green synthesis of iron oxide nanoparticles, assisted by the flower extract. The nanoparticles were synthesized and characterized using UV Visible spectroscopy with characteristic absorbance peaks at 300 nm and 310 nm. Prominent Fourier-Transform Infrared Spectroscopy (FTIR) peaks were obtained corresponding to phenols, amide group, aromatic ring, hydroxyl group, and carbonate ions involved in the stabilization of iron oxide nanoparticles formation. Dynamic light scattering analysis of nanoparticles showed the average sizes as 80.7 nm. Scanning electron microscope images revealed that the size of iron nanoparticles in the range of 160-300 nm. The green synthesized iron nanoparticles have promising potential to inhibit the growth of bacteria. Iron oxide nanoparticles inhibit *E. coli*, *B. subtilis*, *P. aeruginosa* was also enumerated as antimicrobial study. The phytochemicals alkaloid, flavonoid, glycoside, terpenoid, and saponin present in the *Senna auriculata* may be attributed to reducing iron oxide nanoparticles.

**Keywords:** *B. subtilis*, *E. coli*, Iron oxide nanoparticles, *P. aeruginosa* and phytochemical analysis, *Senna auriculata*,

## 1. INTRODUCTION

Nanotechnology is defined as the manufacture of materials and devices on the scale of atoms or small groups of atoms. The “nan scale” is measured in nanometre, or billionths of a meter (nanos, Greek word for “Dwarf”-source of the prefix). The materials built at these scales exhibit distinctive physical and chemical properties because of quantum mechanical effects. Nanotechnology promises greater fuel efficiency in inland transportation, ships, aircraft, and space vehicles.<sup>1</sup> The ongoing worldwide nanotechnology revolution is predicted to impact several areas of biomedical research and other science and engineering applications, including nanoparticles-assisted drug delivery, cell imaging, and cancer therapy.<sup>2</sup> According to the American Society for Testing and Materials (ASTM international 2006), nanoparticles size ranges between 1–100 nm.<sup>3</sup> They have enhanced physical and chemical properties due to the large reactive and exposed surface area with quantum size. They are widely used in many fields such as electronics, photochemical, and biomedicine. They affect as a result of specific electronic structures.<sup>4</sup> Nanoparticles have biomedical applications to deliver pharmaceuticals for both diag-

nostic and therapeutic purposes because they are very small-sized particles. They can also be used for targeted drug delivery, and the metallic nanoparticles respond resonantly to the magnetic field. Surface modification of the nanomaterial has a strong effect on the interaction of these nanomaterials with cells, and it also helps to convert toxic nanomaterial to the less toxic or less toxic to more toxic nanomaterial.<sup>5</sup>

Iron enters the body through the mouth, throat, or digestive tract. The total iron content in adults typically ranges from 3.5 g to 5.0 g. Nearly 20 mg to 25 mg of iron recirculates in our body. The average uptake level of iron in women ranges from 0.040 mg to 0.155 mg per dL of human blood content. For men, it ranges from 0.055 mg to 0.160 mg per dL of human blood level.<sup>6,7</sup> The iron content above the average level in our body leads to hemochromatosis. This is the state in which skin darkens due to the presence of more iron in the bloodstream. Hence the blood is removed from the body, and fresh blood with normal mineral contents is transferred to the body regularly.<sup>9</sup> The iron content below the normal level in our body leads to iron deficiency diseases such as anemia, obesity, and anxiety. This condition shows the inability of the body to take iron from external and

## Corresponding author

C. Narendhar

Email : [narendhar.nano@gmail.com](mailto:narendhar.nano@gmail.com)

Received: 24-04-2021

Accepted: 13-06-2021

Available Online: 01-07-2021

internal sources. This is when the hemoglobin level in human blood gets reduced due to a lack of transferrin-iron bonding because of the low iron level in the body. Blood transfusion is the only way to treat iron deficiency. Hence the iron level should be maintained in the body to keep the body working in average condition.<sup>10</sup>

Iron oxide nanoparticles exist in two forms – one is magnetite ( $\text{Fe}_2\text{O}_4$ ), and another is its oxidized form maghemite ( $\text{Fe}_2\text{O}_3$ ). Iron oxide nanoparticles have super paramagnetic properties, which have a wide range of applications in many fields.<sup>11</sup> Although cobalt and nickel are also high in paramagnetic properties, but they are toxic and easily oxidized. The applications of nanoparticles include the development of terabit magnetic devices, catalysis, sensors, super paramagnetic relaxometry (SPMR), magnetic resonance imaging (MRI), magnetic particle imaging (MPI), magnetic fluid hyperthermia (MFH), separation of biomolecules, targeted drug delivery and targeted gene delivery for medical diagnosis and therapeutics. The nanoparticles are coated by long-chain fatty acids, alkyl-substituted amines, and diols.<sup>12,13</sup> Iron oxide nanoparticles are being used in numerous technologies and incorporated into a wide array of consumer products that take advantage of their desirable optical, conductive, and anti-bacterial properties.

*Senna auriculata* is a leguminous tree. It is commonly known as matura tea tree or avaram. The flower of *Senna auriculata* is the state flower of the state Telangana. It has a wide range of medicinal values.<sup>14</sup> It has cooling property; hence it is used to reduce the elevated body temperature. The decoctions of the flower are used against fever. The phytochemicals present in the flower extract lowers the elevated blood glucose level. Hence, it is used to treat hyperglycemia, which means high glucose level in the bloodstream.<sup>15-17</sup> The seeds of *Senna auriculata* are powdered and applied for conjunctivitis. The antimicrobial along with cooling activity heals eye infections. Because of the presence of high antioxidants in flowers, it keeps our skin and body healthy by neutralizing the free radicals. The leaves of *Senna auriculata* have laxative properties.<sup>18</sup>

## 2. MATERIAL AND METHODS

### 2.1. Materials, Drugs & Reagents

Beaker, conical flask, test tubes, measuring cylinder, glass rod, Petri plates funnel, Wagner's reagent, Meyer's reagent, glacial acetic acid, NaOH, HCl,  $\text{H}_2\text{SO}_4$ ,  $\text{CHCl}_3$ , Potassium hydroxide, Lead acetate, Copper sulfate, Ferric chloride, Nutrient agar, Iodine, Sodium hydroxide, Luria- Bertani broth, Ampicillin, Double distilled water, Sterile distilled water, Ethanol – 70 % & 100%, Laminar

airflow chamber, weighing balance, water-bath, UV Visible spectrophotometer, Fourier transform infrared spectroscopy (FTIR), Dynamic light scattering instrument (DLS), Scanning electron microscope (SEM), centrifuge and micropipettes. Magnetic pellets, centrifuge tubes - 2 mL, 15 mL & 50 mL, cotton plugs, aluminum foil, filter paper, Whatman No 1 filter paper, buds, micropipette tips, cuvette, spatula, *Escherichia coli*, *Bacillus subtilis*, *Pseudomonas aeruginosa*, LB broth, and Nutrient agar.

### 2.2. Synthesis of Iron Oxide Nanoparticles from *Senna auriculata*

The flowers of *Senna auriculata* were collected from Anna University, Trichy, India and authenticated by Dr. M. Palanisamy, Scientist-Incharge, Botanical Survey of India. The collected flowers were washed with tap water to remove the dust content along with it. Then again it is repeatedly washed with Reverse Osmosis (RO) water to remove the unwanted debris. They were shade dried for 5 days in clean environment to naturally dehydrate the water content in it. After 5 days the dried samples were powdered using mechanical blender to obtain dry powder of the extract. Iron oxide nanoparticles were synthesized out by green synthesis method.

5 grams of the powdered sample was mixed with 200 mL of sterile double distilled water and heated at 60°C for 20 minutes. Filter the content with Whatman No.1 filter paper and the extract was stored at -4°C for further uses. Different concentrations of ferric chloride were prepared, made up to a constant volume with sterile double distilled water, and mixed along with the varying volume of flower extract. The precursor ferric chloride was reduced to iron nanoparticles in flower extract; here, the reducing agent is flower extract.

Figure 1 shows the color changes from light brown to black, indicates the formation of iron nanoparticles in the aqueous solution. Then they were centrifuged at 4,000 rpm for 15 minutes at room temperature. The supernatant was discarded, and wash the pellet once with ethanol to remove the impurities. The weight of the pellet was obtained to calculate the optimal nanoparticles synthesis. The high amount of iron nanoparticles were obtained in the 25 mM concentration of ferric chloride precursor and 150 mL of flower extract. The pellet weight

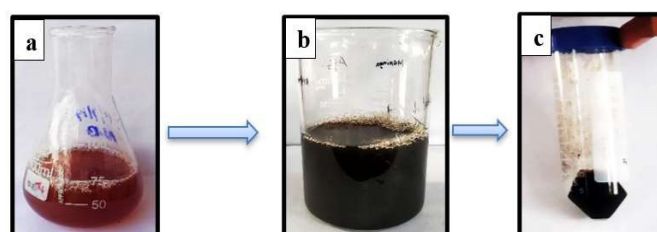


Fig. 1: Synthesis of iron oxide nanoparticles

**Table 1:** Optimization of iron nanoparticles synthesis

S. No.	Ferric chloride	Sterile double distilled water	Flower extract
1	1 M	25 mL	25 mL
2	0.5 M	25 mL	25 mL
3	15 mM	25 mL	25 mL
4	25 mM	25 mL	25 mL
5	35 mM	25 mL	25 mL

of nanoparticles was 400 mg (Table 1). The iron oxide nanoparticles were characterized using DLS and SEM to find the average size and morphology.<sup>19-21</sup>

A: Before nanoparticle formation; B: Black colour appears after nanoparticle formation; C: FeO nanoparticle pellet after centrifugation

### 2.3. Phytochemical Analysis of *Senna auriculata*

Phytochemical screening plays an important role in reducing the extract solution into nanoparticles solution when the particular precursor is added. The presence of phytochemicals like alkaloid was observed by Wagner's Test, flavonoids by alkaline reagent test, saponin by foam test, carbohydrates by Fehling test, and glycosides by Keller Kelliani's test.<sup>22</sup>

### 2.4. Characterization of Nanoparticles

Characterization was done to determine its size and various physical properties using instruments like UV Visible spectrophotometer, FT-IR, DLS and SEM. The distinct peak at a specific nanometer represents the presence of iron oxide nanoparticles. The functional groups attached in the nanoparticles were analyzed by FT-IR analysis. The size of the synthesized nanoparticles was analyzed using DLS method. SEM images give a clear definition to the size of the nanoparticles.<sup>23,24</sup>

### 2.5. Test for Anti-bacterial Activity

The anti-bacterial activities of iron oxide nanoparticles were tested by the agar well diffusion method. The required amount of nutrient agar was prepared in a conical flask using distilled water and sterilized at 121°C for 15–20 minutes, poured into sterile Petri dishes, and allowed to cool for solidification. After confirming the sterility of the agar plates, they were swapped with bacterial isolates evenly over the surface of the agar in the plate. Using the micropipette tips, 4 wells were cut at each petri dish with equal space in-between them. Iron nanoparticles were prepared in the concentration of 20 mg/mL in a 2 mL microcentrifuge tubes. The iron nanoparticles were then introduced into each well. The plates were placed for incubation at 37°C for 24 hrs. After

that, the plates were observed for the zone of inhibition. The zones were measured with a transparent measuring ruler.<sup>25,26</sup>

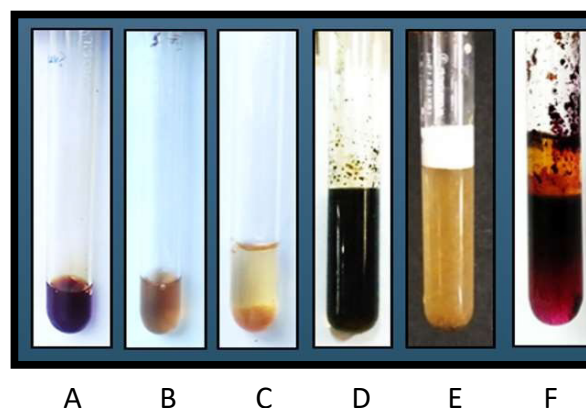
## 3. RESULTS AND DISCUSSIONS

### 3.1. Phytochemical Analysis

Phytochemical analysis was done for the flower extract of *Senna auriculata*. Figure 2 and Table 2 shows that carbohydrates, phenol, and tannin were absent, and alkaloids, flavonoids, glycosides, terpenoids, and saponins were present, which can be confirmed by a color change of extract solution. Studies have shown the presence of secondary metabolites in the extracts of *Senna auriculata*. The phytochemicals play an essential role in reducing the extract solution into nanoparticles solution when the particular precursor is added based on the required nanoparticles.

### 3.2. Morphology Analysis (SEM)

The scanning electron microscope images the sample surface by scanning it with a high-energy beam of electrons in a

**Fig. 2:** Phytochemical result for *Senna auriculata*

A: Alkaloid; B: Flavanoid (NaOH); C: Flavanoid (HCl); D: Glycoside; E: Saponin; F: Terpenoid

**Table 2:** Phytochemical result for *Senna auriculata*

S. No.	Compound	Indication	Inference
1	Alkaloids	Formation of reddish-brown precipitate	+
2	Flavonoids	Appearance of yellow colour	+
3	Saponin	Formation of foam	+
4	Terpenoids	Formation of monolayer of reddish brown colour	+
5	Tannins	Appearance of blue colour	-
6	Phenols	Formation of precipitate	-
7	Glycosides	Appearance of reddish brown colour	+
8	Carbohydrates	Appearance of blue colour	-

'+' indicates presence of phytochemical; '-' indicates absence of phytochemical



raster scan pattern. SEM images clearly show that the morphological smoothers of the iron oxide nanoparticles. Figure 3 shows the size of the nanoparticles was in the range of 160–300 nm.

### 3.3. Particle Size and Zeta Potential Analysis (DLS)

The particle size analysis of the synthesized nanoparticles is done in aqueous reaction media and dry iron oxide nanoparticles dispersed in distilled water using zeta sizer in DLS mode. In Figure 4, it was observed that the average particle size was 80.7 nm which confirmed that the reduction of the metal precursor as nanoparticles since nanoparticles as in the range of 1000 to 1 nm. Hence it was concluded that the average size of the iron nanoparticles were in the range of 80.7nm.

### 3.4. Optical Analysis (UV-Vis)

The nanoparticles were primarily characterized by UV-Vis spectroscopy, which was proved to be a beneficial technique for the analysis of nanoparticles. In UV-Visible spectral analysis, the absorbance spectrum was recorded for 200–800 nm. In Figure 5, a strong peak at 310 nm represents the formation of iron nanoparticles from flower extract in the presence of the precursor ferric chloride. UV-Vis spectrograph of the iron oxide nanoparticles has been recorded as a function of time using a quartz cuvette with water as a reference. In the UV-Vis spectrum, the broadening of the peak indicated that the particles are dispersed.

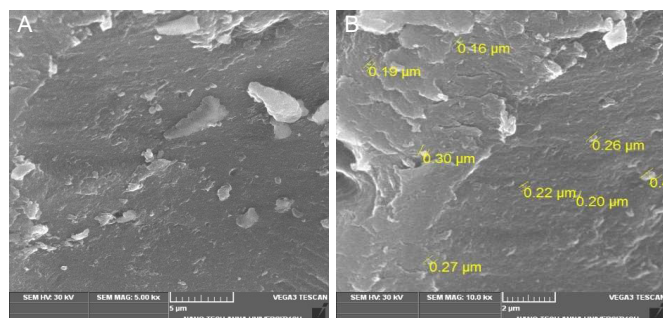


Fig. 3: Morphology analysis (SEM)

A: SEM image of iron nanoparticle – 5 μm; B: SEM image of iron nanoparticle – 2 μm

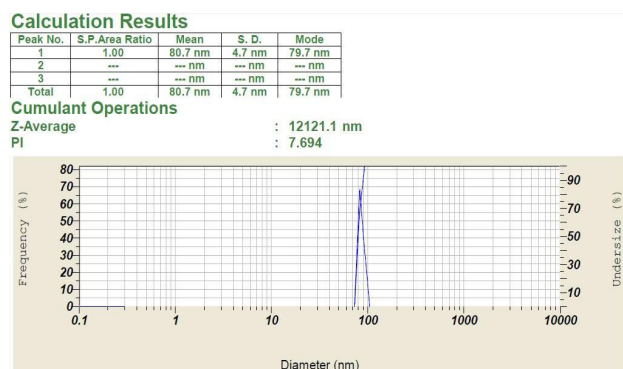


Fig. 4: DLS analysis of iron nanoparticle

### 3.5. Fourier Transform Infrared Spectrum (FT-IR) Analysis

The dry samples of synthesized iron oxide nanoparticles were mixed with potassium bromide (KBr) powder and made into pellet form using Hydraulic pellet press machine and placed in Fourier transform Infra-Red spectrophotometer analysis of the nanoparticles using KBr pellets as reference. Figure 6 shows a strong absorption peak at  $3,425\text{ cm}^{-1}$  indicates the presence of phenols and alcohols with a free O–H group. The peak at  $1,648\text{ cm}^{-1}$  represents the presence of the amide group. The peak at  $1,021\text{ cm}^{-1}$  may be assigned due to the C–O–C group. FT-IR analysis confirmed that the bioreduction of ferric chloride into iron oxide nanoparticles is due to the reduction by capping material of *Senna auriculata* flower extract.

### 3.6. Antimicrobial Assay

Studies on the antibacterial activity of extracts of *Cassia auriculata* extracts were conducted using agar disc diffusion method. The microorganisms used include *Staphylococcus aureus*, *Enterococcus faecalis*, *Bacillus subtilis*, *Salmonella typhi*, *Salmonella paratyphi A*, *Escherichia coli*, *Proteus mirabilis*, *Pseudomonas aeruginosa*, *Klebsiella pneumoniae*, *Vibrio cholera*, and *Shigella dysenteriae*. The maximum activity was observed against all organisms except *Pseudomonas aeruginosa* and *Klebsiella pneumoniae*. The aqueous flower extracts of *Senna auriculata* used to synthesize iron oxide nanoparticles using ferric chloride as the precursor

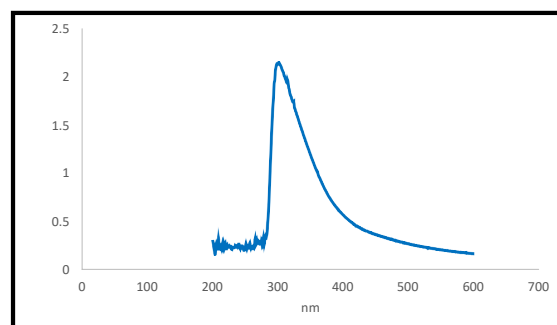


Fig. 5: UV Visible spectrophotometry – FeO Nanoparticle

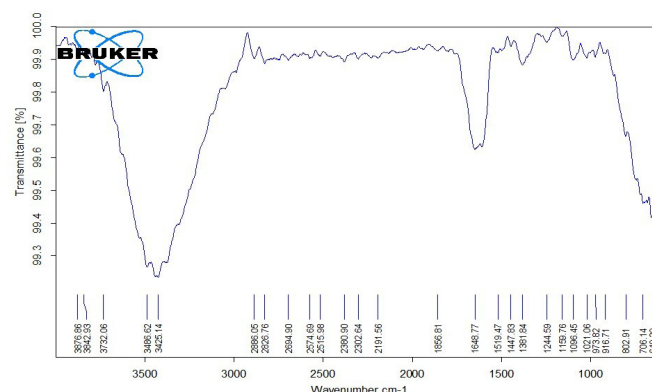


Fig. 6: FT-IR analysis of iron nanoparticle

Table 3: Zone of inhibition against

S. No.	Content	<i>B. subtilis</i>		<i>E. coli</i>		<i>P. aeruginosa</i>	
		Amount ( $\mu$ L)	Zone of inhibition (mm)	Amount ( $\mu$ L)	Zone of inhibition (mm)	Amount ( $\mu$ L)	Zone of inhibition (mm)
1	Antibiotic	30	22	30	10	30	21
2	Distilled water	30	Nil	30	Nil	30	Nil
3	Fe nanoparticles	30	19	30	8	30	17

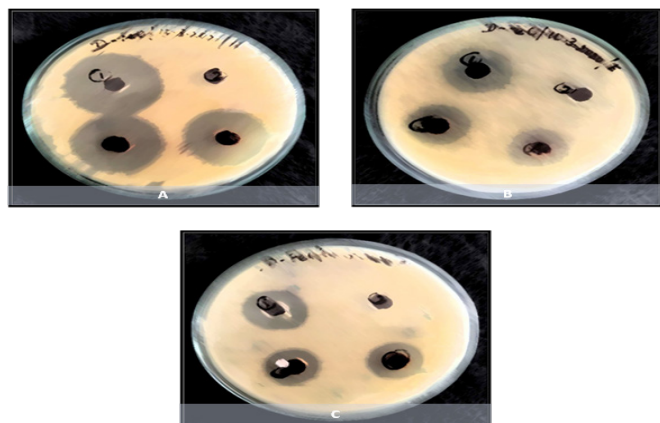


Fig. 7: Antimicrobial assay

A: *B. subtilis*; B: *E. coli*; C: *P. aeruginosa*; 1: Antibiotic; 2: Distilled Water; 3& 4: Fe Np

showed various high zones of inhibition (mm) for many harmful gram-negative and gram-positive bacterial cultures. Anti-bacterial analysis was previously done against *E. coli*, *Bacillus subtilis*, and *Pseudomonas aeruginosa*, which showed various inhibition zones (mm).<sup>27</sup> Figure 7 and Table 3 shows that maximum zone of inhibition attained by Fe Np against *E. coli* was 8 mm, *B. subtilis* was 19 mm and *P. aeruginosa* was 17 mm.

#### 4. CONCLUSION

The present study is important because iron oxide nanoparticle is easily synthesized from *Senna auriculata* flower extract because of the more iron content in the source and shows that the phytochemical analysis of *Senna auriculata* was done using different methods and it shows their presence and absence. Nanoparticles were successfully prepared using the green synthesis method. The formation of nanoparticles was first confirmed by the appearance of black color in the iron nanoparticles. It was characterized in UV-VIS spectroscopy, DLS, FTIR, SEM, and XRD. The average sizes of the nanoparticles were found to be Fe Np – 160 to 300 nm in the SEM analysis. These materials possess different morphology and structural properties. The SEM analysis showed that the aggregation and network formation of nanoparticles had been taking place. Iron nanoparticles have good anti-bacterial activity. Zone of inhibition against *Escherichia coli*, *Bacillus*

*subtilis*, and *Pseudomonas aeruginosa* for iron nanoparticles were 8 mm, 19 mm, 17 mm. These results infer that the Fe nanoparticles have a wide application range and potency.

#### ACKNOWLEDGEMENT

The authors thankfully acknowledge the support from the Department of Biotechnology, Anna University, BIT Campus, Trichy, India. The authors acknowledge the basic research and instruments facility from the Department of Nanoscience & Technology, Sri Ramakrishna Engineering College, Coimbatore, India.

#### REFERENCES

- Chandran M, Yuvaraj D, Christudhas L, et al. Bio Synthesis of Iron Nanoparticles using the brown Seaweed, *Dictyota dictyota*. *Biotechnol Ind J*. 2016;12(12):112.
- Patra JK, Das G, Fraceto LF, et al. Nano based drug delivery systems: recent developments and future prospects. *J Nanobiotechnology*. 2018;16(1):71.
- Jain S, Hirst DG, O'Sullivan JM. Gold nanoparticles as novel agents for cancer therapy. *Br J Radiol*. 2012;85(1010):101-113.
- Jeevanandam J, Barhoum A, Chan YS, Dufresne A, Danquah MK. Review on nanoparticles and nanostructured materials: history, sources, toxicity and regulations. *Beilstein J Nanotechnol*. 2018;9:1050-1074.
- Anderson SD, Gwenin VV, Gwenin CD. Magnetic Functionalized Nanoparticles for Biomedical, Drug Delivery and Imaging Applications. *Nanoscale Res Lett*. 2019;14(1):188.
- Yilmaz B, Li H. Gut Microbiota and Iron: The Crucial Actors in Health and Disease. *Pharmaceuticals (Basel)*. 2018;11(4):98.
- Annibale B, Capurso G, Chistolini A, et al. Gastrointestinal causes of refractory iron deficiency anemia in patients without gastrointestinal symptoms. *Am J Med*. 2001;111(6):439-445.
- Porter JL, Rawla P. Hemochromatosis. [Updated 2021 Mar 29]. In: StatPearls. Treasure Island (FL): StatPearls Publishing; 2021. Available from: <https://www.ncbi.nlm.nih.gov/books/NBK430862/>
- Abbaspour N, Hurrell R, Kelishadi R. Review on iron and its importance for human health. *J Res Med Sci*. 2014;19(2):164-174.
- Jimenez K, Kulnigg-Dabsch S, Gasche C. Management of Iron Deficiency Anemia. *Gastroenterol Hepatol (N Y)*. 2015;11(4):241-250.
- Ali A, Zafar H, Zia M, et al. Synthesis, characterization, applications, and challenges of iron oxide nanoparticles. *Nanotechnol Sci Appl*. 2016;9:49-67.

12. Du Y, Lai PT, Leung CH, Pong PW. Design of superparamagnetic nanoparticles for magnetic particle imaging (MPI). *Int J Mol Sci.* 2013;14(9):18682-18710.
13. Debadin B, Someswar C. Biogenic synthesis of silver nanoparticles using guava (*Psidium guajava*) leaf extract and its anti-bacterial activity against *Pseudomonas aeruginosa*. *Appl Nanosci.* 2016;6:895-901.
14. Surana SJ, Gokhale SB, Jadhav RB, Sawant RL, Wadekar JB. Antihyperglycemic Activity of Various Fractions of *Cassia auriculata* Linn. in Alloxan Diabetic Rats. *Indian J Pharm Sci.* 2008;70(2):227-229.
15. Puranik AS, Halade G, Kumar S, et al. *Cassia auriculata*: Aspects of Safety Pharmacology and Drug Interaction. *Evid Based Complement Alternat Med.* 2011;2011:915240.
16. Kainsa S, Kumar P, Rani P. Pharmacological potentials of *Cassia auriculata* and *Cassia fistula* plants: A review. *Pak J Biol Sci.* 2012;15(9):408-417.
17. Oladeji OS, Adelowo FE, Oluyori AP, Bankole DT. Ethnobotanical Description and Biological Activities of *Senna alata*. *Evid Based Complement Alternat Med.* 2020;2020:2580259.
18. DeFilipps RA, Krupnick GA. The medicinal plants of Myanmar. *PhytoKeys.* 2018;(102):1-341.
19. Bhuiyan MSH, Miah MY, Paul SC, et al. Green synthesis of iron oxide nanoparticle using *Carica papaya* leaf extract: application for photocatalytic degradation of remazol yellow RR dye and anti-bacterial activity. *Heliyon.* 2020;6(8):e04603.
20. Saif S, Tahir A, Chen Y. Green Synthesis of Iron Nanoparticles and Their Environmental Applications and Implications. *Nanomaterials (Basel).* 2016;6(11):209.
21. Imani MM, Safaei M. Optimized Synthesis of Magnesium Oxide Nanoparticles as Bactericidal Agents. *J Nanotech.* 2019;2019:1-6.
22. Gayathri V, Kiruba D. Preliminary phytochemical analysis of leaf powder extracts of *Psidium guajava* L. *Int J Pharmacognosy Phytochem Res.* 2014;6(2):332-334.
23. de Aragão AP, de Oliveira TM, Quelemes PV, PerfeitoMLG, Araújo MC, Santiago J de AS, et al. Green synthesis of silver nanoparticles using the seaweed *Gracilariabirdiae* and their anti-bacterial activity. *Arabian J Chem.* 2019;12(8):4182-8.
24. John Sushma N, Prathyusha D, Swathi G, et al. Facile approach to synthesize magnesium oxide nanoparticles by using *Clitoria ternatea*—characterization and *in vitro* antioxidant studies. *Appl Nanosci.* 2015;6(3):437-444.
25. Kathiraven T, Sundaramanickam A, Shanmugam N, Balasubramanian T. Green synthesis of silver nanoparticles using marine algae *Caulerpa racemosa* and their anti-bacterial activity against some human pathogens. *Appl Nanosci.* 2014;5(4):499-504.
26. Xing TZ, Feng BL. MgO nanoparticles as anti-bacterial agent: preparation and activity. *Brazilian J Chem Eng.* 2010;31(3):591-601.
27. Sudharsana A, Sankari R. Antimicrobial Activity of *Cassia auriculata* Flower Extract on Periodontal Pathogens: An In Vitro Study. *J Pharm Sci Res.* 2017;9(3):267-268.
28. Subhadradevi V, Asokkumar K, Umamaheswari M, Sivashanmugam A, Ushanandhini J, Jagannath P. Antimicrobial Activity of Leaves and Flowers of *Cassia auriculata* Linn. *Bangladesh J Sci Ind Res.* 1970;46(4):513-518.

**How to cite this article:** Priya DD, Rajesh TP, Rachel S, Narendhar C. Iron Oxide Nanoparticles – Characterization and Antimicrobial Studies. *Int. J. Appl. Pharm. Sci. Res.* (2021);6(3): 27-32. doi: <https://doi.org/10.21477/ijapsr.6.3.01>

**Source of Support:** Nil.

**Conflict of Support:** None declared.